Available online at www.sciencedirect.com
ScienceDirect
Applied Geochemistry 22 (2007) 1764–1776
Applied Geochemistry
www.elsevier.com/locate/apgeochem

Geochemistry of Na–HCO_3 groundwater and sedimentary bedrocks from the central part of the Sikhote-Alin mountain region (Far East of Russia)

N.A. Kharitonova *, G.A. Chelnokov, A.A. Karabtsov, V.I. Kiselev

Far East Geological Institute Russian Academy of Science, prospect 100letya 159, Vladivostok 690022, Russia

Available online 24 March 2007

Abstract

New data on major element, trace and rare-earth element (REE) contents of groundwaters and sedimentary bedrock in the Lastochka Spa in the Primorye region of far eastern Russia, together with previous stable isotope data (δD, $\delta^{13}C_{(TIC)}$, and $\delta^{18}O$), allow elucidation of the origin and evolution of groundwater from the spa. The sedimentary bedrock in this area is mainly highly-permeable sandstone. Dominant minerals are K-feldspar, quartz and plagioclase, and secondary minerals are calcite, limonite, sericite and kaolinite. Bedrock samples are enriched in light REE (LREE) and depleted in heavy REE (HREE) and samples where calcite fills the fractures have positive Eu anomalies. Two types of groundwater issue from spring and wells in the study area: fresh water with low mineralization (TDS up to 0.4 g/L) and high pCO_2 water with high mineralization (TDS up to 4.7 g/L). Isotopic data indicate that both types of groundwater are meteoric in origin having a short residence time. Groundwaters are characterized by enrichment of HREE in comparison with LREE and a positive Eu anomaly. Mass balance calculations are consistent with albite dissolution, with or without CO_2 of deep-seated mantle origin as the dominant factor controlling the chemical composition of the groundwater.

1. Introduction

Lastochka Spa is located in the northern part of the Primorye region (Russian Orient Rim) in the south-western part of the Ussuri River catchment not far from the border with China. This spa is well-known in far eastern Russia, and mineral water from the spa is bottled and used widely. Although the existence of the spa has been known for more than a century, the origin of this water, and the role of dissolved CO_2 and water–rock interaction in the geochemical evolution of the water, has not been determined. New data on groundwater chemistry, together with data on the chemical and mineralogical composition of bedrock, enable a detailed assessment to be conducted on the impact of bedrock on the chemical composition of groundwater. Two types of cold groundwater are distinguished in the Lastochka area: (i) fresh groundwater with lower pCO_2 levels, and (ii) groundwater with higher dissolved mineral content and pCO_2 levels. The

* Corresponding author.
E-mail address: tchenat@mail.ru (N.A. Kharitonova).

0883-2927/$ - see front matter © 2007 Elsevier Ltd. All rights reserved.
doi:10.1016/j.apgeochem.2007.03.033

analysis of both water and rock samples are very important to fully understand water–rock interaction. Few previous studies of this area, however, have dealt with both the rock and the groundwaters involved in the water–rock system. Therefore, the mineralogical composition of bedrock, together with geochemistry of major and trace elements, and REEs in groundwater, obtained in this work provide important information on the evolution of water–rock system.

2. Geological setting

The Lastochka Spa is located on the border of the Bikin Cenozoic depression. The oldest formations in the area outcrop on the margins of tectonic blocks in Mesozoic graben structures and consist of Proterozoic crystalline rocks and biotite granite intrusions of Silurian-Devonian age (Fig. 1). In other areas these lithologies are covered by Permian volcano-sedimentary rocks and Triassic-Cretaceous terrigenous formations.

The Lastochka area lies on an anticline that is covered by quaternary clay with a thickness of 1–25 m. Upper Triassic–Middle Jurassic sedimentary rocks plunge with a dip of 40–50°. The central part of the fold is characterized by lower Triassic tuffaceous sandstones, tuffaceous-siltstones, and siltstones; the northwestern part consists of rhythmically layered Middle Jurassic sandstones. Sandstones with silica cement are gray, fine-to-medium grained, and 10–100 m thick. Siltstones are gray to dark gray and 1–10 m thick. Rocks have a good permeability up to a depth of 50–75 m (Sergeev, 1993).

Fig. 1. Geographic setting and geological map of the study area.

The tectonic structure of the Lastochka area is complicated. The deep faults strike NE, many are very deep and served as transport channels for Cretaceous-Neogene mafic to intermediate magmas. The largest structure of this kind is the Buinevichesky Fault (Chelnokov, 1997), which has an angle of dip of 80° and is accompanied by a series of attendant smaller fractures ~50 m thick. The Lastochka area is associated with these faults.

3. Hydrogeological setting

As described in previous hydrological studies (Rinkov, 1988; Chelnokov et al., 1994), the Lastochka area originates from the filling of the Sikhote-Alin' hydrogeological basin (free and artesian aquifers) and the Lower Amur basin (formation water). Two major aquifers are present within the Lastochka area (Fig. 2):

(i) An upper, unconfined aquifer nearest the surface that consists of upper quaternary alluvial sediments – a fine sand, a pebble bed, and a gravel, often with a sandy clay filler. Widespread throughout river valleys, this unit has a thickness of 1–10 m and the maximum depth of the water level in this aquifer is 3 m from the surface. In the Lastochka area, the waters of this aquifer flow towards the Chernaya River.

(ii) A confined aquifer of fractured Jurassic terrigenous sediments that consists of sandstones, siltstones, tuffaceous sandstones and tuffaceous siltstones. Lying either just below the surface or beneath the unconfined aquifer, this unit is $\geqslant$100 m thick. The upper 30–70 m thick fractured zone of this aquifer exhibits good permeability, but in most places is covered by 1–25 m thick clay deposits. Wells discharge about 2–5 l/s, the water is fresh, with a dissolved mineral contents ranging from 200 to 500 mg/L. However, waters with high pCO_2 and mineralization (4000 mg/L) are associated with tectonic fractured zones within this aquifer.

Meteoric waters recharge the multilayered confined aquifer system. Generally, this recharge takes

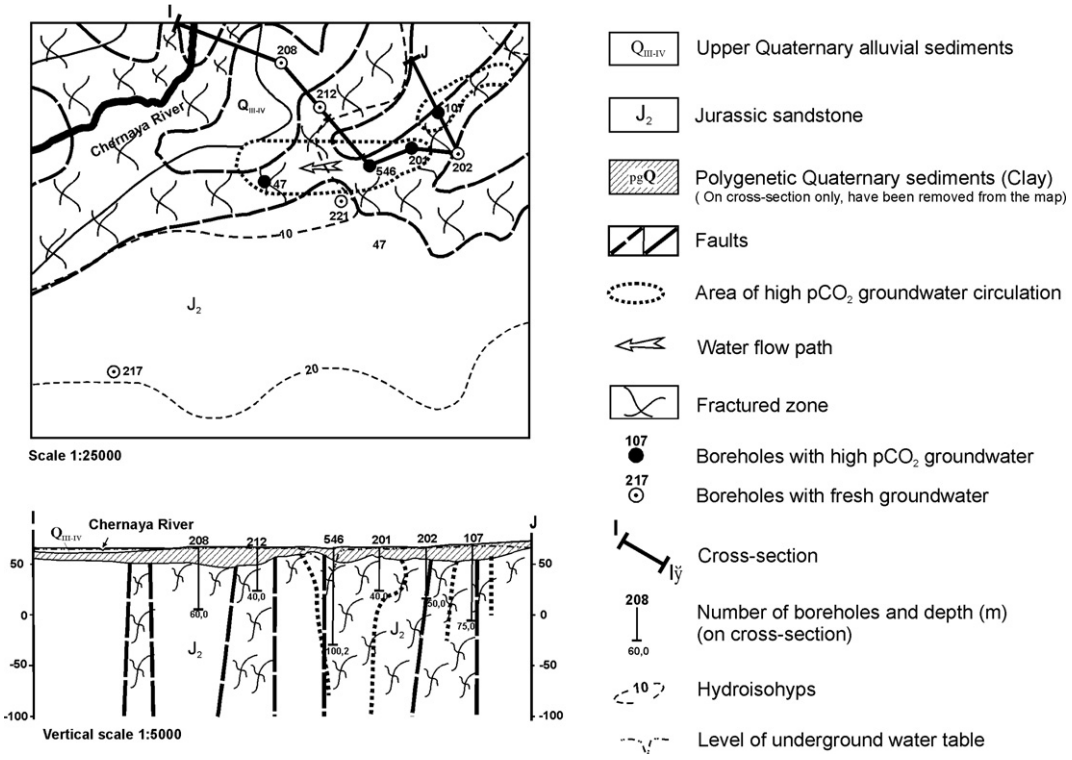

Fig. 2. Hydrogeological map with location of sampling sites and highly schematic hydrogeologic cross-section.

place in areas without a clay cap and in coarse deposits of the alluvial fan located at the edge of the Sikhote-Alin' ridge.

4. Analytical procedures

4.1. Water and gas analysis

Water samples were collected over a 3-a period from boreholes and rivers. The methods used for groundwater sampling, only summarized here, are described in detail by Stetzenbach et al. (1994, 1999) and Johannesson et al. (1997). Groundwater samples were pumped from springs and collected in acid-washed, high-density polyethylene sample bottles. Before sampling, all water samples were passed through 0.45 μm cellulose filters and immediately acidified to pH < 2 with ultrapure HNO_3, excluding samples intended for anion analysis. Water temperature, conductivity, pH, and HCO_3^- content were measured directly in the field, with HCO_3^- determined by titration with 0.1 N HCl.

Major cations and anions were analyzed by ion chromatography. Trace element and REE concentrations in groundwater were determined by ICP–MS (Agilent 4500) analysis at Tokyo University, Japan. Analytical precision for the REEs, except for Ce and Pr, was better than 5% relative standard deviation (RSD); for Ce and Pr, the precision was 9% and 18% RSD, respectively. Stable isotope compositions of waters (D/H and $^{18}O/^{16}O$ ratios) and dissolved CO_2 gas ($^{13}C/^{12}C$ ratios) were determined by isotope-ratio mass spectrometry at the Scientific-Research Institute of Natural Gases and Gas Technologies (VNII-GAZ LLC) in Moscow Measured δD and $\delta^{18}O$ values have analytical precisions of $\pm 1‰$ and $\pm 0.10‰$, respectively. The composition of the gas phase was determined by gas chromatography. Additionally, $\delta^{13}C_{(TIC)}$ data and $C/^3He$ ratios from the previous work of Chudaeva et al. (1999) and additional H- and O-isotope stable isotope data from the literature (Chudaeva et al., 1999) were taken into consideration in this study. Tritium determinations were performed using electrolytic enrichment and subsequent measurement of counting rates; details of sample preparation for ^3H analysis are described by Goriachev (1997). The standard deviation was 1.1–1.6 TU depending on the ^3H concentration.

4.2. Bedrock analysis

The samples of sedimentary bedrock were obtained from cores, which were drilled parallel to hole N546 that was drilled to a depth of 100 m. Core samples of the bedrock for petrographical and mineralogical study were sampled at 5 m intervals. Optical microscopy, classical chemical analysis, X-ray diffraction analysis, electron microprobe chemical analysis, and inductively coupled plasma atomic emission spectrometry (ICP–AES) analysis were used for the characterization of the bulk samples and mineral phases. Multi-element micromapping was undertaken with an electron microprobe (JEOL, JXA-8100) with an EDS INCAx-sight (Oxford, Instruments) in order to provide an image of major and trace element distributions in the samples. Quantitative wavelength dispersive spectrometry (WDS) spot chemical analysis was applied to several minerals and points in the sediment cement. Since C and H were not quantified by the electron microprobe method, the sum of the analyses is less than 100% for CO_2 and H_2O-bearing minerals (carbonates and hydrated phases). X-ray diffraction patterns were obtained on unoriented powder samples using a Dron III diffractometer with a monochromator. Concentrations of Co, Li, Sr and Zr were determined with an ICP–MS (Agilent 7500c). The detection limit for these elements was 0.01 μg/L and the error of the measurement was better than 2% RSD.

To investigate the behavior of REE in different environments (weathered and unweathered zones), two samples were taken for analysis. The subsurface samples were from 15 m depth in the weathered zone and 90 m depth in the unweathered zone. REE abundances were determined by inductively coupled plasma-mass spectrometry (Agilent 7500c). About 0.1 g of each rock sample was decomposed by heating (ca. 180 °C) for more then three days in a teflon vessel with a mixture of $HClO_4$ and HF. The detection limit for REE was 0.01 μg/L and the error of the measurement was better than 5% RSD.

5. Results and discussion

5.1. Mineralogical and element composition of the bedrock

Mineral identification was performed mainly on the basis of microscopic observation and XRD analyses. Optical microscopy indicates that the bedrock of the study area is a uniform stratum consisting mainly of a sandstone of varying grain size. The dominant mineral phases are quartz (>60%), K-feldspar (~15%) and plagioclase (~15%). The abundance of the primary minerals is constant from the surface to deep samples. The sandstones have a good porosity and are often split by fractures up to 10 cm in length that range from 0.5 to 2.0 cm in width. Optical microscopy and XRD analyses indicate that quartz, K-feldspar and plagioclase are present in all samples, with quartz predominant. Sediment cement, which comprises up to 10% of the rock volume, is mainly quartz and hydromica. The full mineralogical composition of the bedrocks is presented in Table 1. Generally, chlorite and clay minerals such as kaolinite, smectite and illite are the most common secondary minerals in the fault, but the total amount of clay present in samples examined during this study does not exceed 10% of the rock volume. XRD data indicate that kaolinite is more abundant than other clay minerals and its abundance depends slightly on the depth within the cored section. The samples collected up to 20 m depth that represent the weathering zone have 4.5 times more kaolinite than samples from the unweathered zone at 100 m depth. Although only a trace of dolomite was detected by the XRD analyses, thin veins filled with secondary carbonate minerals such as siderite and calcite were observed by microprobe analysis in samples collected below 30 m depth. In rock samples at a depth of 90–100 m from the surface, the macro-fractures are filled mainly with carbonate minerals. Zircon, rutile, sphene, leucoxene, anatase and tourmaline are accessory minerals.

Full chemical compositions of some mineral phases are given in Table 2 and the points of microprobe analysis are indicated in Fig. 3a and b. The K-feldspar is a clear orthoclase containing thin veins of a Na-plagioclase. The surface of the orthoclase grains is unweathered. Quantitative spot chemical analyses show that the orthoclase contains a small amount of Na (0.4–1.2% Na_2O), Ba (up to 0.55%), and Fe (up to 0.42%). The plagioclase is albite with a low content of Ca (0–2.7% CaO) and K (0–3.5% K_2O). From the surface to a depth of 20 m, the core is highly fractured and weathered; with the fractured surfaces covered with Fe-oxides due to alteration. Dots and veins of Fe-mineral, diagnosed in thin section as limonite, were observed in this zone (Fig. 3b). However, a detailed study of the Fe-mineral indicates that it is Fe(II) oxyhydroxide with large amounts of Mg (6.7–7.8% MgO) and a small amount of Ca (0.5–1.04% CaO). Albite is

Table 1
Mineralogical characteristics of the bedrock (counting in thin section, volume%)

Samples	Depth (m)	Quartz	K-Feldspar	Plagioclase	Micas	Clays	Carbonate	Pyrite	Fe-oxide
Fine-grained sandstone	11	60	15	13	–	9	–	–	3
Medium-grained sandstone	15	60	15	13	–	9	–	–	3
Coarse-grained sandstone	20	60	15	14	–	9	–	–	2
Coarse-grained sandstone	25	60	15	15	5	5	–	–	–
Coarse-grained sandstone	30	60	15	15	5	5	–	–	–
Coarse-grained sandstone	35	60	15	15	5	5	–	–	–
Medium-grained sandstone	40	60	15	15	5	5	–	–	–
Medium-grained sandstone	45	60	15	15	5	5	–	–	–
Medium-grained sandstone	50	60	15	15	5	5	–	–	–
Medium-grained sandstone	55	60	15	15	5	5	–	–	–
Medium-grained sandstone	60	60	15	15	5	5	–	–	–
Fine-grained sandstone	65	60	15	15	5	4	–	1	–
Fine-grained sandstone	70	60	15	15	5	4	–	2	–
Fine-grained sandstone	75	60	15	15	4	4	–	2	–
Fine-grained sandstone	80	60	15	15	4	3	–	4	–
Fine-grained sandstone	85	60	15	15	3	2	–	5	–
Fine-grained sandstone	90	60	15	17	3	2	3	–	–
Fine-grained sandstone	95	60	15	17	3	2	3	–	–
Fine-grained sandstone	100	60	15	17	3	2	3	–	–

Table 2
Chemical analysis of bedrock minerals by microprobe (wt%)

Minerals	Points	Na	K	Al	O	Ca	Ba	Si	Mg	Fe	Total
K-Feldspar	1	0.91	11.19	9.98	46.09	–	0.49	29.75			98.41
	2	0.35	12.28	9.78	46.06	–	–	29.90	–	0.33	98.69
	3	0.39	12.12	9.94	45.86	–	–	29.61	–	–	97.91
Plagioclase	4	6.91	–	10.21	46.38	–		31.07			97.57
	5	7.00	–	10.34	49.94	–		31.56			98.85
	6	5.35	2.95	10.53	49.72	1.92	–	30.15	–	–	98.70
	7	5.69	0.13	10.91	46.88	1.96		29.70			95.27
Kaolinite	8	0.26	1.23	18.70	47.70			21.89	0.18	0.37	90.35
	9	0.33	0.31	17.54	46.76	–	–	22.78	0.33	0.44	88.50
	10	0.45	2.74	16.84	43.92	–	–	22.66	0.36	0.53	87.51
Carbonate	11	–	–	–	43.78	25.03	–	–	4.35	11.89	85.44
	12	–	–	–	40.77	22.13	–	–	4.69	13.21	81.07
Fe-hydroxide	13	–	–	–	30.89	0.75	–	–	4.74	37.24	74.92
	14	–	–	–	30.97	0.38	–	–	4.05	39.61	75.31

the most altered mineral of the sedimentary bedrock, whereas the surface of quartz and orthoclase is almost unweathered. A grain of the albite, completely transformed to a clay mineral, is shown in Fig. 3b. This observation is in good agreement with calculations of the lifetime of 1 mm crystals at pH 5 for various minerals studied by Lasaga (1984). His data indicate that albite dissolves 6.5 times faster than orthoclase and 425 times faster than quartz. Based on microprobe analysis and XRD data, this clay mineral is kaolinite. Cubes of pyrite are widespread in the interval from 65–85 m depth. It is noteworthy that the amount of this mineral increases with depth. The microprobe analyses permit the identification of two generations of pyrite; one strongly weathered (Fig. 4a) and a more recent one having a nodular structure (Fig. 4b). Several grains of apatite with a considerable amount of F (4.83–5.14 wt%) were observed in some samples by electron microprobe analysis. These minerals can contain up to 0.92 wt% of Yb.

The sandstone unit displays a relatively consistent chemical composition (Table 3). The distribution of some major and minor elements in the sandstone is indicated in Fig. 5. A weak P_2O_5 and TiO_2 enrichment was observed for the upper part of profile. The content of TiO_2 decreases from the upper to lower zone, reaching a minimum of 0.12 wt% at 60 m depth. The diminution TiO_2 content observed is probably due to the lack of a Ti-bearing

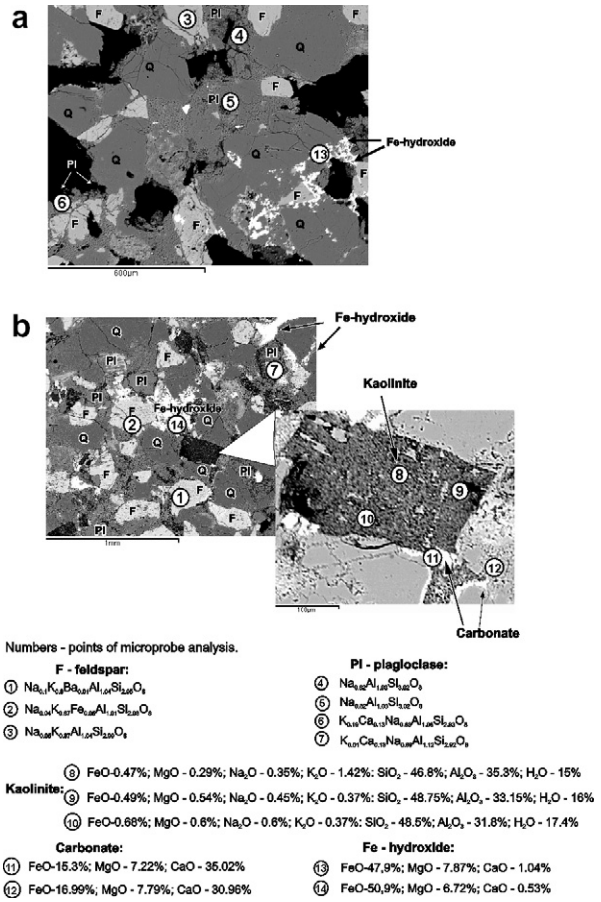

Fig. 3. General view of high porous sandstone from bedrock of Lastochka spa (a) and surface of dominated mineral assemblage with example of almost completely transformed albite grain (b). Photos obtained using microprobe analyzer Jeol, JXA 8100 in COMP mode.

mineral. Contents of Na_2O significantly decrease with depth, which may indicate the alteration of primary albite to kaolinite and leaching of Na. Aluminium and K_2O concentrations slightly increase with depth, ranging from 12.2–20.7 wt% and 4.42–6.37 wt%, respectively. Phosphorus contents decrease to 0.08 wt% with increasing depth, with the presence of P-bearing minerals the likely cause of the elevated P_2O_5 near the surface. Enrichment of Co from 50 to 85 m is likely the result of the replacement of Fe by Co in the structure of pyrite which is prominent in this interval. Zirconium concentration exhibits a slight increase with depth from 2.7 to 5.2 ppm (Fig. 5), whereas the contents of Li and Sr decrease downward from 16.5 to 8.1 ppm and 130 to 115 ppm, respectively. Zirconium contents depend mainly on the amount of zircon present. Optical microscopic and electron microprobe data indicate that small grains of zircon, ranging in size from 1 to 20 μm diameter, are widespread throughout the bedrock. The content of HfO_2 in zircon does not exceed 0.33–1.3%. Elevated contents of Li and Sr in the upper part of profile are a result of the leaching these elements during alteration of primary silicate at depth and subsequent aqueous transport toward the surface and co-precipitation in newly-formed clay minerals.

5.2. REE in the bedrock

The REE concentrations in two samples of the sedimentary bedrock taken from weathered and unweathered zones are shown in Table 4 and chon-

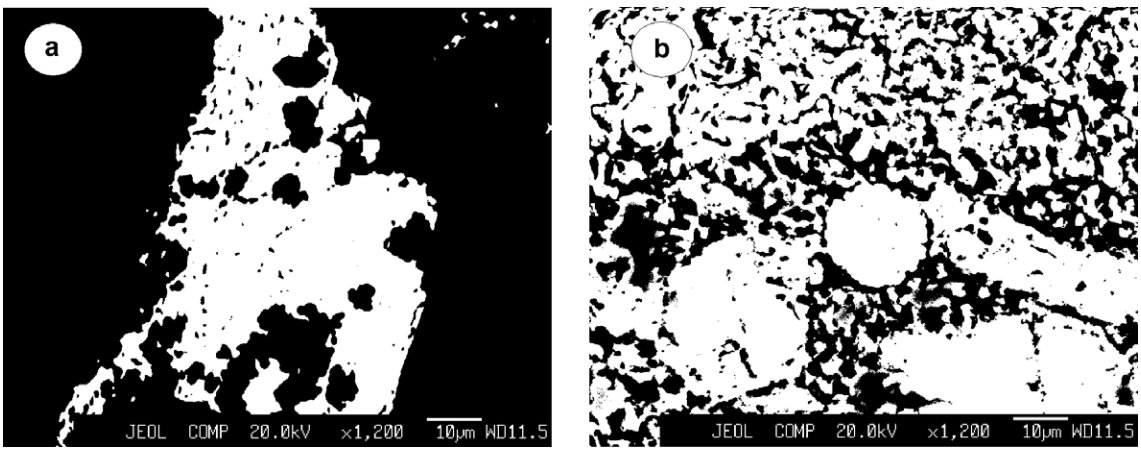

Fig. 4. Two generations of pyrite: (a) strongly weathered, (b) probably new-forming with nodules structure.

Table 3
Chemical composition of bedrock (in wt% of dried sample)

Depth (m)	10	20	30	40	50	60	70	80	90	100
SiO_2	76.8	72.4	69.3	73.0	72.3	78.0	74.6	71.7	70.4	63.7
TiO_2	0.45	0.28	0.25	0.23	0.22	0.12	0.27	0.23	0.28	0.25
Al_2O_3	12.2	14.0	15.0	15.0	15.3	14.8	15.1	16.2	15.9	20.7
Fe_2O_3	1.05	0.35	0.90	0.15	–	0.30	0.92	–	1.22	0.50
FeO	0.49	1.39	2.2	0.62	1.51	0.6	0.52	0.54	0.39	1.2
MnO	–	0.13	0.11	–	0.02	–	0.05	–	0.07	0.04
MgO	0.2	0.32	0.31	0.21	0.5	–	0.2	–	0.41	0.82
CaO	0.42	0.6	0.43	–	0.69	0.7	0.28	1.3	0.58	0
Na_2O	1.54	2.60	2.52	1.35	2.09	3.00	1.64	1.36	1.87	1.71
K_2O	4.42	4.48	4.87	5.05	4.85	4.60	4.70	5.10	5.14	6.37
P_2O_5	0.18	0.15	0.09	0.15	0.06	0.05	0.08	0.11	0.10	0.08
H_2O^-	0	0.2	0.1	0.3	0	0	0.3	0	0.3	0
H_2O^+	2.31	2.68	3.4	3.59	2.08	1.5	2.8	3.4	2.8	3.96
Sum	100	99.7	99.5	99.7	99.6	103.7	101.5	99.9	99.5	99.3
Be, ppm	1.80	2.30	1.60	2.60	5.20	3.00	2.10	2.80	4.50	–
Co, ppm	3.30	4.30	3.50	4.00	5.20	6.10	6.60	7.00	7.50	–
Cr, ppm	14.2	22.0	10.7	22.3	24.7	19.5	16.0	21.6	27.8	–
Cu, ppm	7.64	9.88	7.20	8.73	6.33	5.16	6.13	4.18	6.90	–
Li, ppm	16.5	13.5	10.3	6.75	9.05	9.09	7.02	9.08	8.10	–
Pb, ppm	44.1	47.6	49.0	49.0	49.0	51.1	49.0	56.0	35.0	–
Sr, ppm	130	126	135	160	123	120	118	118	115	–
Zn, ppm	32.9	60.5	46.2	66.2	73.6	48.5	45.7	82.2	43.6	–
Zr, ppm	2.73	2.63	1.65	3.45	4.14	2.00	2.58	2.94	5.16	–

Note: – = not analyzed.

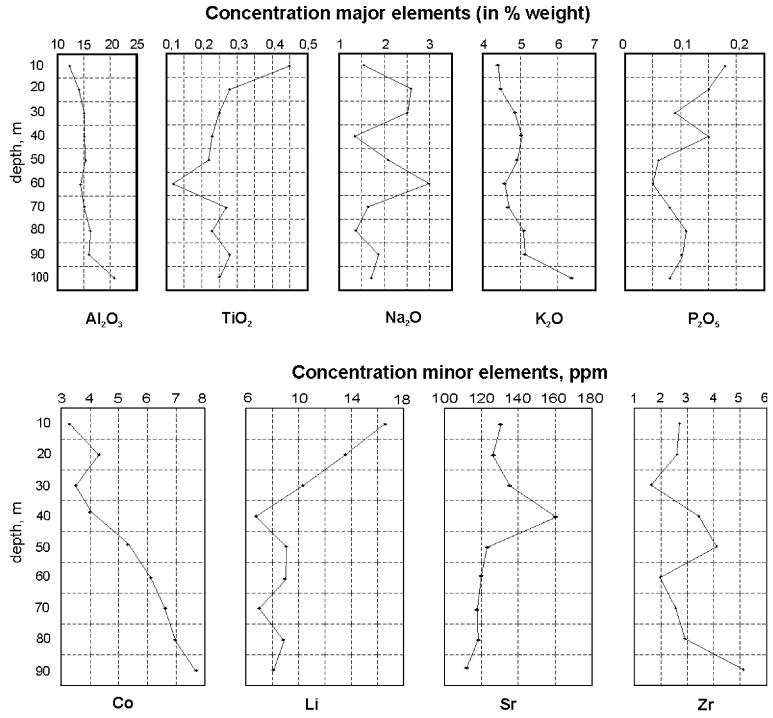

Fig. 5. Profiles of distribution several major and minor elements in bedrock of Lastochka spa.

Table 4
REE concentration in bedrock (ppm) and groundwater (ng/L)

	Sample rock at 90 m depth	Sample rock at 15 m depth	High pCO_2 groundwater	Fresh groundwater
La	35	131	41	81
Ce	53	221	14	94
Pr	4.4	10.1	2	10
Nd	18.2	44	90	118
Sm	3.8	9.8	31	36
Eu	0.94	1.6	159	105
Gd	2.35	6.5	66	70
Tb	0.35	1.0	20	–
Dy	1.41	3.7	127	136
Ho	0.32	0.83	13	16
Er	1	2.4	176	188
Tm	0.18	0.44	20	–
Yb	0.99	2.32	158	173
Lu	0.14	0.31	16	18
LREE	115	418	338	447
HREE	6.7	17.5	489	529

drite-normalized REE patterns displayed in Fig. 6. Both rock samples are strongly enriched in light REE and depleted in heavy REE, with La/Yb varying from 3.4 to 5.5. The REE abundance in the weathered sample at 15 m depth is three times greater than in the unweathered sample from 90 m depth. Such enrichment in the REE content is likely to have been caused both by precipitation of REE in clay minerals, which are abundant at this depth, and adsorption on the Fe-oxides precipitated from groundwater at shallow depths. Y/Ho ratios for both rock samples are very similar, 13.3 in the unweathered rock and 13.5 in the weathered rock, however these Y/Ho ratios differ strongly from the chondritic value of 28.1. The NASC-normalized REE patterns of both samples are characterized by a strong negative Dy anomaly and positive Tm anomalies, but a positive Eu anomalies was observed only in the REE pattern of the unweathered sample collected from 90 m depth. In this sample, the macro-fractures are filled by carbonate, not clay. Because plagioclase is strongly enriched in Eu, the occurrence of positive Eu anomalies is generally considered to reflect the presence of plagioclase (Taylor and McLennan, 1988). This explanation does not explain the positive Eu anomaly in the Lastochka area sedimentary rocks. Both the weathered and unweathered sandstone have the same mineralogical composition, differing only in the presence of calcite and Fe-oxide (Table 1). However, the observed Eu depletion observed in the weathered sandstone is consistent with results from leaching experiments (Lee et al., 2004), which noted that positive Eu anomalies were observed only in gneissic rock cores where calcite was the main fracture-filling mineral. Therefore, the positive Eu anomaly for the Lastochka sandstone can be explained by co-precipitation of Eu with calcite derived from groundwater.

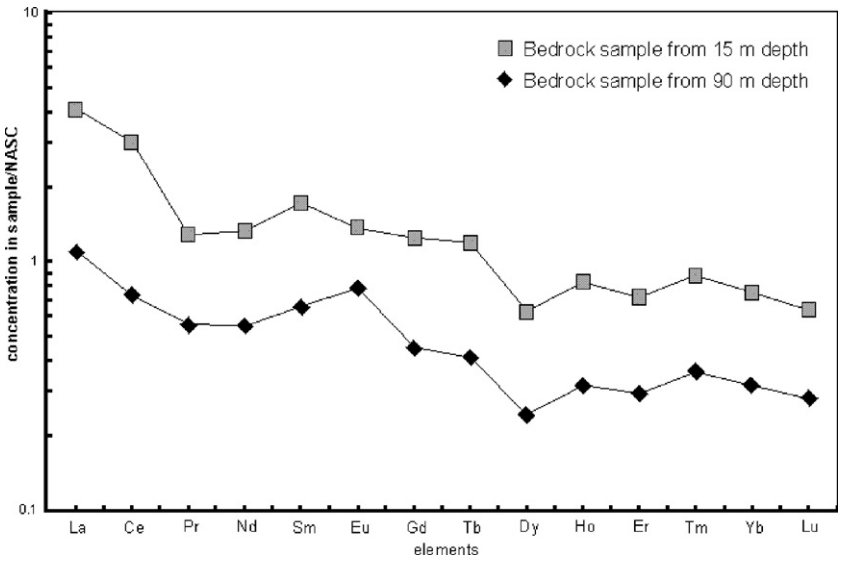

Fig. 6. NASC (North American Shale Composite) normalized concentrations of rare earth elements in two samples of bedrock. NASC data were taken from Hannigan and Sholkovitch (2001).

Table 5
Hydrochemical data for studied waters (mg/L)

Borehole	Water type	pH	TDS	Na	K	Ca	Mg	Fe	NH_4	Cl	SO_4	HCO_3	SiO_2	F
208	Fresh	7.5	313	26.2	2.0	34.0	17.0	0.1	–	5.7	4.0	159	61.5	0.12
212	Fresh	7.4	380	20.7	1.9	50.1	18.2	0.1	–	8.5	4.0	244	26.9	0.2
217	Fresh	7.5	420	38.6	3.0	42.1	17.1	0.1	–	7.1	16.0	268	24.6	0.1
221	Fresh	7.3	400	33.1	2.9	34.1	14.6	0.1	–	4.3	2.0	246	53.9	0.6
201	High pCO_2	6.3	1460	90.2	4.0	173	70.5	4.0	–	4.3	10.0	1122	38.5	–
546	High pCO_2	6.7	3650	520	57.4	184	150	0.69	0.6	4.3	6.0	2684	38.7	0.08
107	high pCO_2	6.3	3562	400	52.0	153	107	10	0.2	27	2.0	1939	32.3	–
47	high pCO_2	6.0	4974	530	86.9	220	163	2.4	–	8.8	8.2	3111	–	–

– Not determined.

5.3. Water geochemistry

Groundwater samples were collected over a 3-a period; additionally some data from Fomin et al. (1977) and Chudaeva et al. (1999) were considered and re-interpreted during this study. Sample locations are indicated on Fig. 2. Two types of groundwater are distinguished in the study area (Table 5): (i) a fresh water with low mineral content (TDS levels that range from 313 to 400 mg/L) having nearly a constant HCO_3^- content of about 240 mg/L and very slightly alkaline pH values of 7.3 to 7.5; and (ii) a high-CO_2 water (TDS levels range from 1460 to over 4900 mg/L) having a HCO_3^- content ranging up to almost 5000 mg/L and more variable and slightly acidic pH values of 6.0 to 6.7. Both types of water belong to the Na–Ca–HCO_3^- type and are used as a source of potable bottled water. Springs monitored during a complete annual cycle revealed that both types of groundwater showed that no significant temporal variation occurs in the chemical composition of either groundwater type. The high-pCO_2 waters are enriched in Fe, most likely due to dissolution of pyrite and siderite in these slightly acidic waters. The saturation indices of these mineral obtained using the WATERQ4F computer code (Ball and Nordstrom, 1991) indicates that the waters are strongly undersaturated with respect to the pyrite and slightly undersaturated with respect to siderite. The correlation observed on plots of Na–HCO_3^- (Fig. 7a) and TDS–HCO_3^- (Fig. 7b) indicate that the Na content and TDS value in groundwater directly depend on the concentration of HCO_3^-. This can be explained by dissolution of the primary Na-bearing aluminosilicate phase albite at elevated CO_2 gas pressures. It is well known that the presence of dissolved CO_2 enhances the extent of water–rock interactions, especially at low temperature (Criaud and Fouillac, 1986; Greber, 1994). Therefore, the addition CO_2 gas to a groundwater should increase water–rock interaction and result in more intense element leaching from the bedrock. Thermodynamic calculations indicate that the waters of the Lastochka Spa area are strongly undersaturated with respect to the primary aluminosilicate minerals albite and anorthite. However, detailed study of the grain surface by microprobe analysis clearly shows that only albite, not anorthite, is the weathered mineral. Mass balance calculations using NETPATH (Plummer et al., 1991) indicate that the most important reaction controlling the chemical composition of both types of groundwater in the Lastochka Spa area is dissolution of albite in the presence or absence of CO_2 gas. Only a minor amount of orthoclase and mica are dissolved. Calcite and kaolinite precipitation accompany the albite dissolution.

Thermodynamic data indicate that both types of groundwater examined in this study are in equilibrium with respect to calcite, dolomite, quartz and chalcedony, but are supersaturated with respect to kaolinite, mica, hematite and goethite. Moreover, the fresh water is slightly undersaturated with respect to Ca-smectite and siderite. A stability diagram indicates that data for the CO_2-charged waters fall within the stability field of kaolinite, whereas the freshwater data fall on the boundary of the kaolinite-Ca-smectite stability fields.

Hydrogen (δH) and O (δ^{18}O) isotopic data (Chudaeva et al., 1999) indicate that local meteoric precipitation is the ultimate source of both water types. In the classical δD vs. δ^{18}O diagram, all the CO_2-rich mineral water in Primorye region lies on or close to the global meteoric water line (Craig, 1961). Consequently, the dominant processes controlling chemical composition of these waters is gas–water and water–rock interaction. The ^{3}H value measured in the high-pCO_2 groundwater is 5.3

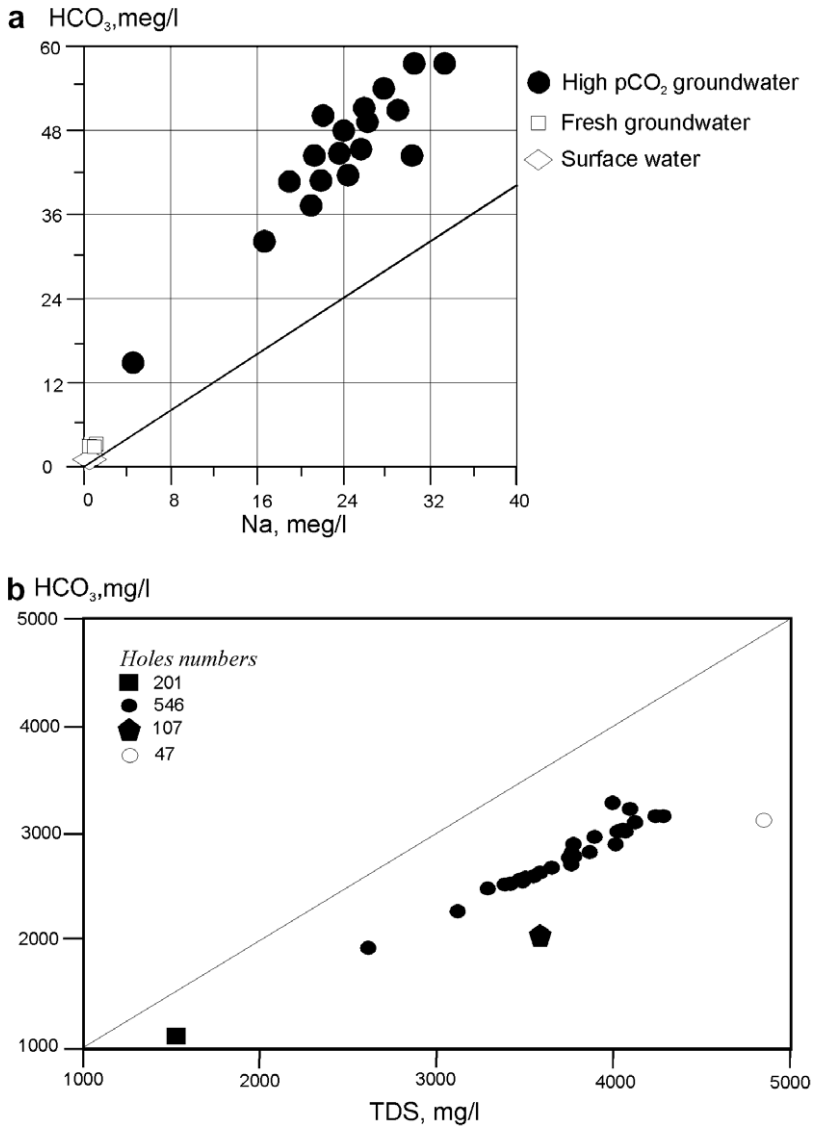

Fig. 7. Correlation between concentrations: (a) sodium and bicarbonate ions, (b) TDS bicarbonate ions in groundwater from Lastochka spa.

tritium units (TU), compared to 29.3 TU for the surface water of the Ussiry River. Thus, the deep groundwater of the Lastochka Spa area is modern, post-1952 water.

5.4. Gas geochemistry

The main gas constituent in the high-pCO_2 groundwater is CO_2, which may represent as much as 98% of the total amount of dissolved gas. The CO_2 partial pressure, calculated using data obtained from the water analyses is about 0.6 atm, whereas that measured in the field reached as high as 2.6 atm. The pressure of CO_2 in shallow, low-conductivity freshwaters is 10^{-2} atm. Free CO_2 of Lastochka Spa waters have $\delta^{13}C_{PDB}$ values of about −6.2‰. According to Chudaev et al. (2001), the $\delta^{13}C$ values for total inorganic C in the cold CO_2-charged groundwater of the region range between −8.2 and −4.2‰, suggesting a deep-seated mantle origin for the most of CO_2 in the studied waters. The similarity in C-isotope composition for the free CO_2 of Lastochka Spa waters suggests a similar source for the C, with the high-CO_2 waters resulting

from migration of gas from the mantle to the surface through the deep faults present across the region. Additional $C/^3He$ data support this hypothesis (Chudaeva et al., 1999).

5.5. The REE data of the groundwater

For high-pCO_2 groundwater, the total REE content ($\sum$REE+Y) is 1.1 as compared to 1.5 μg/L for the low-conductivity freshwaters. Shale-normalized REE plots for both types of groundwater from Lastochka Spa are presented in Fig. 8, together with REE data from the other spas and springs of the Sikhote-Alin mountain range region taken from Shand et al. (2004). All waters are relatively enriched with respect to middle and heavy REE, although the waters represented in Fig. 8 are present in different types of bedrock lithologies. In the case of Lastochka Spa, both types of groundwater also are enriched in middle and heavy REEs compared to LREEs, although the opposite was observed in the bedrock samples. Furthermore, the biggest difference in LREE and HREE contents was observed in the more mineralized, high-pCO_2 waters. For example, Yb/La ratios are 3.82 for the high-pCO_2 waters but only 2.12 for the dilute groundwater. This may be due to preferential aqueous transport of HREE, which are known to form stronger aqueous carbonate complexes than LREE. Previous work has shown that HREE are more strongly complexed by carbonate than LREE (Cantrell and Byrne, 1987) and therefore, LREE are more easily sorbed onto particles or colloids (Byrne and Sholkovitz, 1996). The HREE enrichment and LREE depletion of parent rocks compared to groundwaters are probably the result of preferential leaching of the HREEs from minerals during water–rock interaction (Balashov et al., 1964; Ronov et al., 1967; Nesbitt, 1979; Duddy, 1980) and retention of LREEs. Therefore, the aqueous solution would be enriched by HREEs during water–rock interaction, whereas LREEs are mainly concentrated in the residual rock or secondary mineral phases.

The Y/Ho ratio is 20.5 and 29.5 for the high-pCO_2 and dilute groundwater, respectively, very

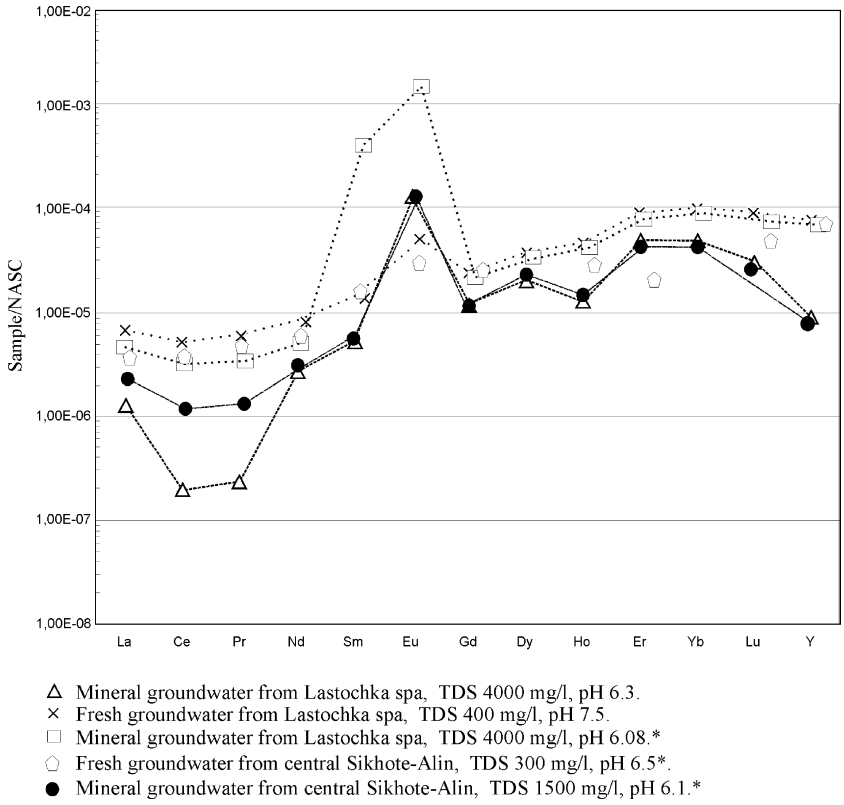

Fig. 8. NASC (North American Shale Composite) normalized concentrations of REE in the studied groundwater from Lastochka spa. NASC data were taken from Hannigan and Sholkovitch (2001). *, marked data taken from Shand et al. (2004).

close to both the parent rock and the chondritic values. A strong negative Ce anomaly is clearly observed for high-pCO_2 water, but is less pronounced for the dilute groundwater. This feature most likely results from oxidative scavenging of Ce from solution onto Mn-oxyhydroxides (Koeppenkastrop and De Carlo, 1993; DeCarlo et al., 1998) or, albeit less likely, onto Fe-oxyhydroxides. Although the former authors showed conclusively that Mn-oxyhydroxides can cause oxidation of Ce(III) to insoluble Ce(IV) and its removal from solution, Bau (1999) suggested that uptake of Ce onto Fe oxyhydroxides can also occur. The latter author has reported that this is a relatively slow process; hence the variations in the magnitude of observed Ce anomalies can result from difference in the time of interaction between water and bedrock. All samples of groundwater from this study have a distinct positive Eu anomaly that is in good agreement with the data of Shand et al., 2004 who described the distribution of REE in several high-pCO_2 waters in the Primorye region.

According to Nelson et al. (2004), positive Eu anomalies may develop in two ways: the bedrock could have an unusually high content of Eu or groundwater with positive Eu anomalies might reflect considerably more reduced conditions in parts of the aquifer. The presence of positive Eu anomalies in the water could also indicate weathering of plagioclase (Taylor and McLennan, 1988). The Lastochka Spa waters circulate in a sedimentary bedrock with moderate concentrations of REE (Table 4). However, plagioclase, which concentrates Eu, is the principal mineral constituent in this rock. Because plagioclase dissolves faster than quartz and K-feldspar, its predominance could account for the enrichment of Eu in the groundwater. It remains unclear, however, why no difference in Eu content is observed in groundwaters of different pCO_2, contents, because CO_2 partial pressure differences should affect the dissolution rate of plagioclase. Dissolution of zircon would also produce the observed enrichment of groundwater in HREEs; however, it is generally accepted that zircon is stable during low-temperature weathering.

6. Summary and conclusions

Analysis of sedimentary rocks and groundwater from the Lastochka Spa located in the central part of the Sikhote-Alin mountain range in far eastern Russia lead to the following conclusions:

1. Both types of groundwater (low- and high-pCO_2) originate from local meteoric precipitation and variable extents of water–rock interaction has played a dominant role in the development of the chemical signatures of the waters. Isotopic data indicate that CO_2 gas in the groundwater may be mantle derived and its presence is critical for the development of the high-pCO_2 groundwater. This type of groundwater evolves only during gas–water/water–rock interaction. Extensive dissolution of albite in the presence of CO_2 gas leads to a lower pH and considerable accumulation of dissolved mineral constituents, leading to a high Na content in the high-pCO_2 water. Lastochka Spa area waters appear to have a short subsurface residence time, both being post-1952 waters on the basis of the ^3H content. The strong contrast between the trace element concentrations of both waters is caused by more intensive weathering of primary minerals in the deep water due to the presence of elevated CO_2 contents. Fault systems that define the areas of highly-mineralized water circulation appear to play an important role in CO_2 migration to the surface.
2. REE data indicate that the sedimentary bedrock is enriched in HREEs and depleted in LREEs, whereas the groundwaters are enriched in HREE in comparison to LREE. This observation can be explained largely by the preferential leaching of the HREEs from sedimentary bedrock during water–rock interaction in the presence of CO_2. Positive Eu anomalies observed in the fractured sandstone are probably caused by precipitation of calcite from groundwater. This hypothesis is supported by the saturation indices of minerals, which show that both types of groundwaters are in equilibrium with calcite. Positive Eu anomalies are present in both types of water and probably reflect extensive weathering of albitic plagioclase in the presence of CO_2.

Acknowledgements

We would like to thank Dr. O.V. Chudaev for his helpful comments and Dr. V.A. Chudaeva for assistance in measurement of REEs in groundwaters. We are grateful to the FEB RAS (project 06-III-A-08-323) and Russian Scientific School Foundation (No. 9542.2006.5) for funding our investigation. We also thank Dr. R.S. Harmon, Dr. R. Fuge and anonymous external reviewers, who made valuable suggestions for improving the paper.

References

Balashov, Y.A., Ronov, A.B., Migdisov, A.A., Turanskaya, N.V., 1964. The effect of climate and facies environment on the fractionation of the rare earth elements during sedimentation. Geochem. Int. 5, 951–969.

Ball, J.W., Nordstrom, D.K., 1991. User's manual for WATERQ4F with revised thermodynamic data base and test cases for calculating speciation of minor, trace and redox elements in natural waters. U.S. Geol. Surv. Open File Rep., 91–183.

Bau, M., 1999. Scavenging of dissolved yttrium and rare earths by precipitating iron oxyhydroxides: Experimental evidence for Ce oxidation, Y-Ho fractionation, and lanthanide tetrad effect. Geochim. Cosmochim. Acta 63, 67–77.

Byrne, R.H., Sholkovitz, E.R., 1996. Marine chemistry and geochemistry of lanthanides. In: Gschneider, K.A., Jr., Eyring, L. (Eds.), Handbook on the Physics and Chemistry of Rare Earths, 23. Elsevier, Amsterdam, pp. 97–593.

Cantrell, K.J., Byrne, R.H., 1987. Rare earth element complexation by carbonate and oxalate ions. Geochim. Cosmochim. Acta 51, 597–605.

Chelnokov, A.N., 1997. Groundwaters in Primorye region: Distribution and forming condition. PhD thesis, Institute of Earth Crust RAN RAS, Irkutsk (in Russian).

Chelnokov A.N., Chelnokova B.I., Druzhinina M.V., Alekseenko O.I. 1994. Results of regional estimation forecast resources of mineral water in Primorye region. In: Russian. Hydrogeology Report Series of the Russian Geological Survey, Vladivostok.

Chudaev, O.V., Chudaeva, V.A., Sugimori, K., Nagao, K., Takano, B., Matsuo, M., Kuno, A., Kusakabe, M. 2001. New geochemical data of the high PCO_2 waters of Primorye (Far East Russia). In: Proceedings of the Tenth International Symposium on Water Rock Interaction, WRI-10, 473–477.

Chudaeva V.A., Chudaev O.V., Chelnokov A.N., Edmunds W.M., Shand P., 1999. Mineral waters of Primorye (chemical aspect). Vladivostok, Dalnauka (in Russian with English summary).

Craig, H., 1961. Isotopic variations in meteoric waters. Science 133, 1702–1703.

Criaud, A., Fouillac, C., 1986. Étude des eaux thermominérales carbogazeuses du Massif Central Français II. Comportment de quelques métaux en trace, de l'arsenic, de l'antimoine et du germanium. Geochim. Cosmochim. Acta 50, 1573–1582.

DeCarlo, E.H., Wen, X.Y., Irving, M., 1998. The influence of redox reactions on the uptake of dissolved Ce by suspended Fe and Mn oxide particles. Aquatic Geochem. 3, 357–389.

Duddy, I.R., 1980. Redistribution and fractionation of the rare-earth and other elements in a weathering profile. Chem. Geol. 30, 363–381.

Fomin, F.F., Vasiliev, N.E., Kniajev, V.A., 1977. Some features of hydrochemical regime of Lastochka spa. Proc. Balneotherapy in Far East of Russia. Magadan, 32–35.

Goriachev, V.A., 1997. Development and adaptation of the high sensitive gas proportion method of tritium measurement for oceanic purpose. PhD thesis. Pacific Oceanic Institute of Far East Brunch of RAS. Vladivostok (in Russian).

Greber, E., 1994. Deep circulation of CO2-rich palaewaters in a seismically active zone (Kuzuluk/Adaparazi, northwestern Turkey). Geothermics 23, 151–174.

Hannigan, R.E., Sholkovitch, E.R., 2001. The development of middle rare earth elements enrichments in freshwater weathering of phosphate minerals. Chem. Geol. 175, 495–508.

Johannesson, K.H., Stetzenbach, K.J., Hodge, V.F., Kreamer, D.K., Zhou, X., 1997. Delineation of ground-water flow systems in the southern Great Basin using aqueous rare earth element distributions. Ground Water 35, 807–819.

Koeppenkastrop, D., De Carlo, E.H., 1993. Uptake of rare earth elements from solution by metal oxides. Environ. Sci. Technol. 27, 1796–1802.

Lasaga, A.C., 1984. Chemical kinetics of water–rock interactions. J. Geophys. Res. 89, 4009–4025.

Lee, S.-G., Kim, Y., Chae, B.-G., Koh, D.-C., Kim, K.-H., 2004. The geochemical implication of a variable Eu anomaly in a fractured gneiss core: application for understanding Am behavior in the geological environment. Appl. Geochem. 19, 1711–1725.

Nelson, B.J., Wood, S.A., Osiensky, J.L., 2004. Rare earth element geochemistry of groundwater in Palouse basin, northern Idaho-eastern Washington. Geochem. Explor. Environ. Anal. 4, 227–241.

Nesbitt, H.W., 1979. Mobility and fractionation of rare earth elements during weathering of a granodiorite. Nature 279, 206–210.

Plummer, K.N., Prestemon, E.C., Parkurst, D.L., 1991. An interactive code (Netpath) for modeling net geochemical reactions along a flow path. US Geol. Surv. Water. Resour. Investig., 91–4078.

Rinkov, V.S., 1988. Underground water of Far East. Hydrogeology Report Series of the Russian Hydrogeological Survey, Vladivostok.

Ronov, A.B., Balashov, Y.A., Migdisov, A.A., 1967. Geochemistry of the rare earth elements in the sedimentary cycle. Geochem. Int. 4, 1–17.

Sergeev, I.V., 1993.Geological structure and ore deposit in the low flow interfluve of Bikin and Bolshaya Ussurka rivers. Report. 277 (in Russian).

Shand, P., Johannesson, K.H., Chudaev, O., Chudaeva, V., Edmunds, W.M., 2004. Rare earth contents of high pCO2 groundwaters of Primorye, Russia: Mineral stability and complexation controls. Rare Earth Elements in Groundwater Flow Systems. Springer, pp. 161–186.

Stetzenbach, K.J., Amano, M., Kreamer, D.K., Hodge, V.F., 1994. Testing the limits of ICP–MS: Determination of trace elements in ground water at the parts-per-trillion level. Ground Water 32, 976–985.

Stetzenbach, K.J., Hodge, V.F., Guo, X., Farnham, I.M., Johannesson, K.H., 1999. Using multivariate statistical analysis of groundwater flow in regional aquifer. Hydrol. Proc. 13, 2655–2673.

Taylor, S.R., McLennan, S.M., 1988. In: Gschneider, K.A., Jr., Eyring, L. (Eds.), Handbook on the Physics and Chemistry of Rare Earths, 11. Elsevier, Amsterdam, pp. 485–578.